Brain Imaging and Behavior
DOI 10.1007/s11682-016-9597-3

ORIGINAL RESEARCH

Altered functional connectivity within and between the default model network and the visual network in primary open-angle glaucoma: a resting-state fMRI study

Jieqiong Wang[1,2] · **Ting Li**[3] · **Peng Zhou**[1,2] · **Ningli Wang**[4] · **Junfang Xian**[3] · **Huiguang He**[1,2,5]

Abstract To explore the alterations of functional connectivity (FC) and connections within and between the subnetworks of the visual network and the default mode network in glaucoma. We applied the independent component analysis to obtain two resting-state networks (RSNs), which were the visual network and the default mode network (DMN), from the resting-state fMRI data of 25 primary open-angle glaucoma (POAG) patients and 25 well-matched normal controls. Then FC analysis was performed to obtain the altered FC within the RSNs, whereas the functional network connectivity (FNC) analysis was performed within and between these two RSNs. The abnormalities were correlated with clinical measures in glaucoma to investigate the abnormality-clinical relationship. FC analysis showed that the FC in the occipital pole of the visual network was decreased in POAG patients while no alterations were found in the FC of the DMN in patients. FNC analysis of connections within the RSNs found that two of the three connections within the visual network were decreased while no connection alterations were found within the DMN. FNC analysis of connections between these two RSNs found two increased connections and one decreased connection. The decreased connection between these two RSNs was positively correlated with the visual field mean deviation. These findings shed light on the importance of the reorganization of resting state networks in glaucoma mechanism, which may facilitate the understanding of glaucoma.

Keywords Subnetwork · Independent component analysis · Glaucoma · Functional connectivity · Functional network connectivity

Electronic supplementary material The online version of this article (doi:10.1007/s11682-016-9597-3) contains supplementary material, which is available to authorized users.

✉ Junfang Xian
cjr.xianjunfang@vip.163.com

✉ Huiguang He
huiguang.he@ia.ac.cn

[1] State Key Laboratory of Management and Control for Complex Systems, Institute of Automation, Chinese Academy of Sciences, Beijing, China

[2] University of Chinese Academy of Sciences, Beijing, China

[3] Department of Radiology, Beijing Tongren Hospital, Capital Medical University, Beijing, China

[4] Department of Ophthalmology, Beijing Tongren Hospital, Capital Medical University, Beijing, China

[5] Center for Excellence in Brain Science and Intelligence Technology, Chinese Academy of Sciences, Beijing, China

Introduction

Glaucoma is the second leading cause of blindness in the world and its mechanism is controversial. Previous studies have shown that glaucoma is more like a neurodegenerative disease rather than just an eye disease (Gupta et al. 2006a; Gupta and Yucel 2007), since the damage of central visual system (Garaci et al. 2009; Gupta et al. 2006b; Dai et al. 2011) and that of other brain regions (Dai et al. 2013; Frezzotti et al. 2014; T. Li et al. 2015; Williams et al. 2013) are found in glaucoma patients. Although a bunch of studies have revealed the structural changes (Williams et al. 2013; W. W. Chen et al. 2013; Yu et al. 2013) and functional alterations (Song et al. 2014; T. Li et al. 2015) of the brain in glaucoma patients via magnetic resonance imaging (MRI), only a few studies focused on the functional communication between brain regions, which constitutes the basis for complex brain functions.

Published online: 04 October 2016

The overall organization of functional communication is usually measured by the conventional whole-brain network or sparsity-based network. The investigation of the reorganization of the brain network pattern in glaucoma has shown that although the efficiency of functional communication is preserved in the brain network of glaucoma at the global level, the efficiency of functional communication is altered at the local level (Wang et al. 2016a, b). This points out the importance of examining the functional communication between specific brain regions.

The functional communication between specific brain regions is usually investigated either by the seed-based method or by the independent component analysis (ICA). With the seed-based method, researchers created functional connectivity (FC) maps based on a prior-defined region (seed) and found FC alterations in the visual cortex of glaucoma patients (Dai et al. 2013). However, this method is heavily sensitive to the prior-defined region and cannot eliminate the noise effect even though noise correction is performed (Murphy et al. 2009).

In contrast to the seed-based FC, ICA overcomes the aforementioned problems, and can clearly distinguish within- and between-network connectivity (Joel et al. 2011; von dem Hagen et al. 2012). The ICA method divides the whole-brain voxels into different components (or spatial maps), within which the voxels are highly synchronously co-activated (van de Ven et al. 2004). The components are identified as different resting-state networks (RSNs) based on their brain functions (Damoiseaux et al. 2006; van den Heuvel and Hulshoff Pol 2010), such as the salience network, the visual network, the default mode network (DMN), etc. The components in one RSN can be called as the subnetworks of this RSN. Recently, Frezzotti et al. have revealed the FC abnormalities within and outside the visual network of glaucoma via ICA (Frezzotti et al. 2014). However, this study only focused on the alterations of functional connectivity within the subnetworks, and did not explore the alterations of functional connections between the subnetworks (components) of the same RSN or those of different RSNs.

Since glaucoma is a disease with vision impairment, the study of functional connectivity within the visual network in glaucoma is of great importance to understand the brain alterations of glaucoma. DMN is one of the most important resting-state networks, which includes the medial prefrontal cortex, the posterior cingulate cortex, ventral anterior cingulate cortex, precuneus and inferior parietal lobe (Raichle et al. 2001). The brain regions of DMN are active when the subject is at rest state but suppressed when carrying out different tasks (Greicius et al. 2003). Moreover, DMN alterations were found in the patients with schizophrenia (Ongur et al. 2010), social anxiety disorder (Gentili et al. 2009), et al. The DMN overlaps considerably with brain regions targeted by Alzheimer's disease (Alba et al. 2004; Vidal et al. 2004), which is the commonest complication of glaucoma. Although Frezzotti's study did not find FC alterations in the DMN of glaucoma patients, functional abnormalities in the DMN of glaucoma patients have been revealed in another study (T. Li et al. 2015). Hence, DMN also contributed to the brain alterations in POAG patients.

In the current study, we investigated the alterations of FC within subnetworks as well as the abnormal connections between subnetworks in the visual network and the DMN. We utilized ICA to obtain the visual network and DMN, followed by FC analysis and functional network connectivity (FNC) analysis. Finally, we correlated the alterations with clinical measures.

Materials and methods

Subjects

This retrospective study was approved by the Medical Ethics Committee of the Beijing Tongren Hospital, and all subjects have signed the informed consent. From 2009 and 2012, 25 primary open angle glaucoma (POAG) patients (age: 44.6 ± 13.0 years, male/female: 11/14) and 25 age- and gender-matched healthy subjects (age: 36.8 ± 11.6 years, male/female: 13/12) were recruited by Beijing Tongren Hospital. The age match of two groups was identified by a two-sample t test ($p = 0.071$) while the gender match of two groups was identified by a chi-squared test ($p = 0.778$). To make glaucoma diagnosis objective and in a blinded manner, three glaucoma clinicians independently conducted a series of ophthalmologic examinations, including optic intraocular pressure, gonioscopy, fundoscopy and standard automated perimetry.

After glaucoma diagnosis, the patients in the following cases were excluded: (1) with any other visual diseases or any psychiatric disorder, (2) using drugs that may influence brain function, (3) using alcohol or nicotine within 3 months. We excluded those normal controls which have (1) any visual disease or any psychiatric disorder, (2) drugs that may influence brain function, and (3) alcohol or nicotine within 3 months. No subjects were excluded in the current study.

Data acquisition

The hospital applied a GE 3 T scanner to obtain the rsfMRI data and T1-weighted imaging of participants. The scanner parameters of rsfMRI data were: TR/TE = 2000/35 ms, slice thickness = 5 mm, flip angle =90°, matrix =64 × 64, FOV = 24 × 24 cm^2, yielding 28 axial slices. The scanner parameters of T1-weighted imaging were: TR/TE = 8.9/3.5 ms, slice thickness = 1 mm, flip angle =13°, matrix =256 × 256, FOV = 24 × 24 cm^2, yielding 209 axial slices.

Three clinical measures were used to reflect glaucoma severity: visual field loss (mean deviation: MD), cup-to-disk ratio (CDR), and retinal nerve fiber layer (RNFL) thickness.[1] Typically, a small visual field MD (a high CDR) represents a high degree of severity on glaucoma. The visual field MD was measured by 30–2 Swedish Interactive Testing Algorithm (SITA) fast visual field tests with standard automated perimetry (Humphrey Field Analyzer; Zeiss Meditec AG, Jena, Germany). The CDR and RNFL thickness were measured by the iVue 100 (Optovue Inc., Fremont, California, USA). Note that when collecting the medical records for this retrospective research, some clinical data were missing because the patients' recruitment date (between 2009 and 2012) was a long time ago. Finally, there were 14 POAG patients have complete clinical parameters (see Table S1 in the supplementary materials).

Subnetwork analysis

Figure 1 shows the pipeline of subnetwork analysis in POAG patients. After standard preprocessing of all participants' imaging data, we applied group ICA on the rsfMRI data to obtain two RSNs, i.e. the visual network and the DMN. Subsequently, FC analysis and FNC analysis were performed on the subnetworks of these two RSNs. Finally, we correlated the resulting abnormalities with clinical parameters of POAG to investigate the relationship between the abnormalities of subnetworks and the severity of glaucoma. The details are as follows.

Preprocessing

A MATLAB toolbox DPARSF (V2.3, http://www.restfmri.net/forum/taxonomy/term/36) (Yan and Zang 2010) was applied to conduct the standard preprocessing of the rsfMRI data. The standard preprocessing has been described in many previous studies (Dai et al. 2013; Tian et al. 2012). In short, the preprocessing included slice correction, head realignment, spatial normalization to MNI space, resampling to 3 mm isotropic voxels, smooth (4 mm full width at half maximum Gaussian kernel), linear detrend, band-pass filtering, and the regression of nuisance covariate effects.

Group independent component analysis

Group independent component analysis of the preprocessed data was performed by the toolbox GIFT (Version 3.0a,http://mialab.mrn.org/software/gift/index.html) (Bell and Sejnowski 1995). In the group ICA analysis, we used the minimum description length criteria (Y. O. Li et al. 2007) to estimate the number of components of all subjects (number of subjects: M), resulting in 31 components. Figure 2 showed the pipeline of group ICA, which included single principle component analysis (PCA), group PCA, ICA and back reconstruction. We carried out the group ICA on the data of both normal controls and POAG patients to ensure that all subjects had the same components. Firstly, the single PCA was performed on the preprocessed data $\mathbf{Y}_i (1 \le i \le M)$ to get the reduced data $\mathbf{Y}_i^* (1 \le i \le M)$. Then, we concatenated the reduced data $\mathbf{Y}_i^* (1 \le i \le M)$ and performed the group PCA on the concatenated data to further reduce the dimension. The infomax-based ICA algorithm (Bell and Sejnowski 1995) was conducted on the result of the group PCA $\mathbf{X}$ to obtain the components of the group $\widehat{\mathbf{S}}$ (spatial map) and the corresponding time course $\widehat{\mathbf{A}}$. Finally, we utilized the ICA results and the information of PCA to perform the back reconstruction (Calhoun et al. 2001; Erhardt et al. 2011) of the individual subject's spatial map $\tilde{\mathbf{S}}_i \ (1 \le i \le M)$ and corresponding time course $\tilde{\mathbf{R}}_i (1 \le i \le M)$. The definition of mathematical variables used in group ICA is offered in Table 1.

Identification of the visual network and the DMN

GIFT could automatically label the components corresponding to the visual network and the DMN by a template-matching algorithm. In brief, the templates of 14 resting state networks including the visual network and the DMN were provided by GIFT (Shirer et al. 2012). Each component was spatially correlated with the offering templates. The best template was selected based on the maximum correlation value. Considering that the recruited population characteristics (e.g., age range, gender distribution, etc.) of participants in our study may differ from those of participants used in the creation of the template, two anatomical experts were asked to further identify the visual network and the DMN.

Functional connectivity analysis

We performed z-score transformation on the components of the visual network and DMN to improve the normality of the components. Then two-sample t tests were applied to compare the components (subnetworks) of two groups with age and gender as covariates. Cluster-wise false-discovery rate (FDR) correction ($p < 0.001$) was used to perform multiple testing corrections.

Functional network connectivity analysis

We conducted functional network connectivity (FNC) analysis with FNC toolbox, a supplementary toolbox to GIFT. FNC analysis focused on the temporal correlation between the

[1] Practically, more emphasis should be put on visual field MD and CDR than RNFL.

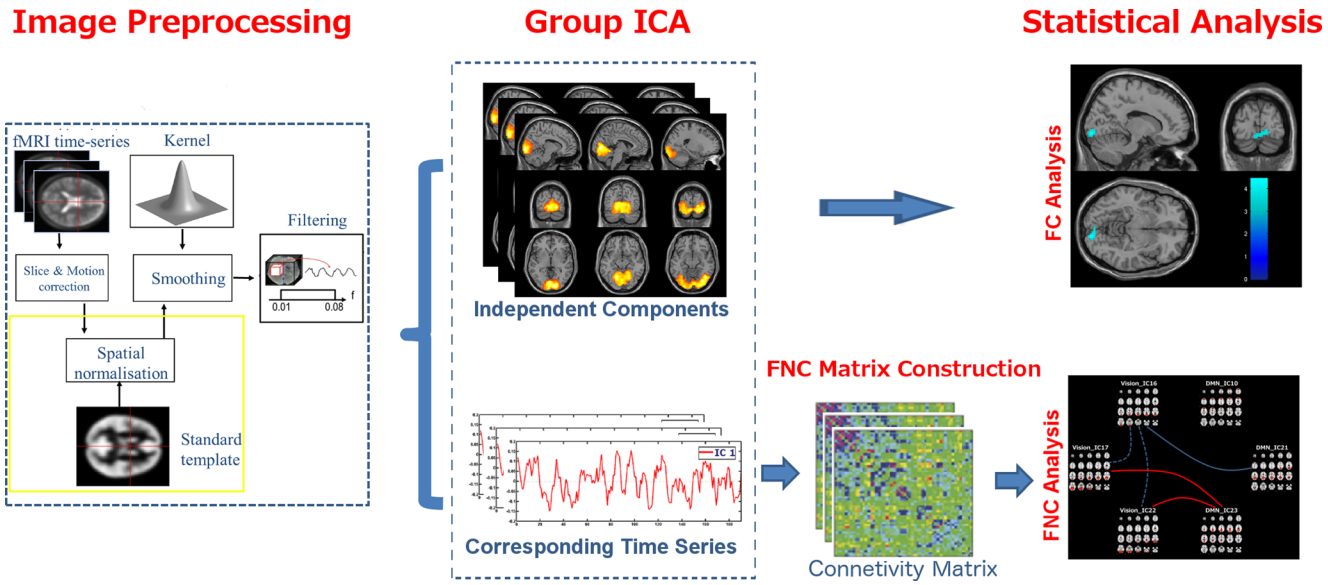

Fig. 1 The pipeline of subnetwork analysis in POAG patients

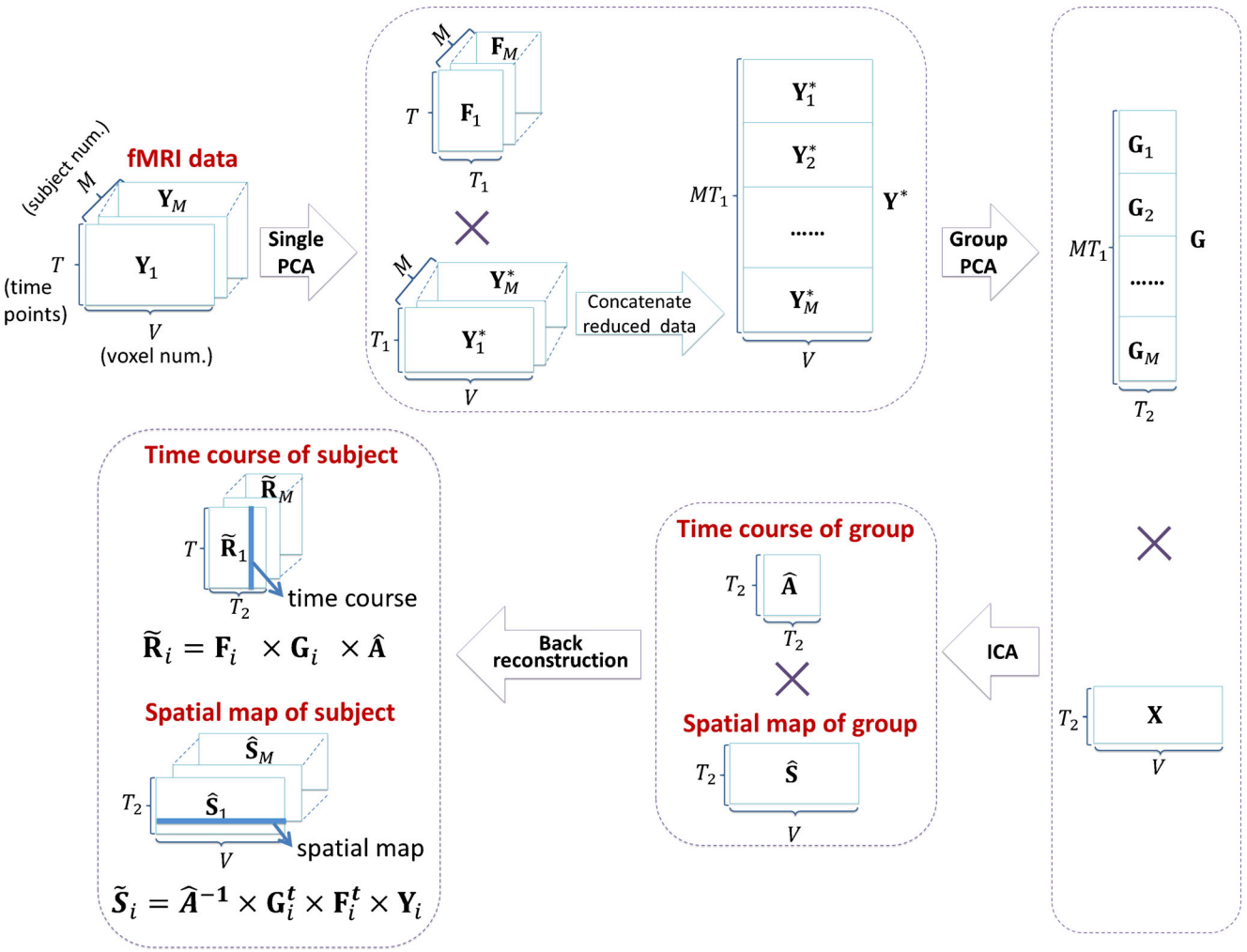

Fig. 2 The pipeline of Group ICA

Table 1 The definition of mathematical variables used in group independent component analysis

Variables	Definition
M	The number of subjects
V	The number of voxels in the preprocessed fMRI data
T	The time points of the 4D preprocessed fMRI data
$\mathbf{Y}_i$ $(i = 1, 2, \cdots, M)$	The preprocessed fMRI data matrix ($T \times V$) of subject i
T_1	The number of principle components retained for each subject in the process of single PCA
$\mathbf{Y}_i^*$ $(i = 1, 2, \cdots, M)$	The reduced data matrix ($T_1 \times V$) after single PCA of subject i
$\mathbf{F}_i$ $(i = 1, 2, \cdots, M)$	The standardized reducing matrix ($T \times T_1$) of subject i in the process of single PCA ($\mathbf{Y}_i = \mathbf{F}_i\mathbf{Y}_i^*$)
$\mathbf{Y}^*$	The time-concentrated data matrix ($MT_1 \times V$) of all subjects ($\mathbf{Y}^* = \left[\mathbf{Y}_1^{*t}, \mathbf{Y}_2^{*t}, \cdots, \mathbf{Y}_M^{*t}\right]^t$)
T_2	The number of principle components retained in the process of group PCA
$\mathbf{X}$	The reduced data matrix ($T_2 \times V$) after group PCA
$\mathbf{G}$	The standardized reducing matrix ($MT_1 \times T_2$) in the process of single PCA ($\mathbf{Y}^* = \mathbf{G}\mathbf{X} = \left[\mathbf{G}_1^t, \mathbf{G}_2^t, \cdots, \mathbf{G}_M^t\right]^t\mathbf{X}$, $\mathbf{Y}_i^* = \mathbf{G}_i\mathbf{X}$)
$\widehat{\mathbf{S}}$	Spatial map ($T_2 \times V$) of the group of whole subjects obtained by ICA
$\widehat{\mathbf{A}}$	Time course or mixing matrix ($T_2 \times T_2$) of the group of whole subjects obtained by ICA ($\mathbf{X} = \widehat{\mathbf{A}}\widehat{\mathbf{S}}$)
$\tilde{\mathbf{S}}_i$ $(i = 1, 2, \cdots, M)$	Spatial map ($T_2 \times V$) of subject i after back reconstruction ($\tilde{\mathbf{S}}_i = \widehat{\mathbf{A}}^{-1}\mathbf{G}_i^t\mathbf{F}_i^t\mathbf{Y}_i$)
$\tilde{\mathbf{R}}_i$ $(i = 1, 2, \cdots, M)$	Time course ($T \times T_2$) of subject i after back reconstruction ($\tilde{\mathbf{R}}_i = \mathbf{F}_i\mathbf{G}_i\widehat{\mathbf{A}}$)

components (subnetwork) obtained by ICA, which was evaluated by computing the maximal lagged correlation coefficient $\delta_{\mathbf{XY}}$ between each pair of subnetworks (Jafri et al. 2008):

$$\delta_{XY} = \max_{-t \le \Delta i \le t}\left(\frac{\boldsymbol{X}_{i_0}^T\boldsymbol{Y}_{i_0+\Delta i}}{\sqrt{\boldsymbol{X}_{i_0}^T\boldsymbol{X}_{i_0}}\sqrt{\boldsymbol{Y}_{i_0+\Delta i}^T\boldsymbol{Y}_{i_0+\Delta i}}}\right) \quad (1)$$

where $\mathbf{X}$ and $\mathbf{Y}$ were the corresponding time courses of two subnetworks, respectively, i_0 was the reference time points of two subnetworks, Δi was the lag time, the maximal lag time t = 2TR. We calculated all 6 × (6–1)/2 = 15 pair-wise combinations and then conducted one-sample t tests to determine the significance of combination ($p < 0.05$, FDR corrected). Two-sample t tests were subsequently applied to detect the abnormal connections within the subnetworks and between the subnetworks with age and gender as covariates.

Relationship with clinical measures

We correlated the abnormal FC and abnormal network connectivity coefficients with the visual field MD and the CDR to investigate the relationship with the clinical parameters of glaucoma (the 14 patients with complete parameters), controlling for age, gender and intracranial volume (ICV). This correlation analysis was conducted in the SPSS software (release 17.0), and the relationship was significant if the p-value was below 0.05.

Results

Identification of the visual network and the DMN

The brain was divided into 31 independent components (IC) by group ICA analysis. After the spatial correlation with network template and the identification of experts, three independent components, IC 16, IC 17 and IC 22 (correlation coefficients: 0.344, 0.262 and 0.350), were identified as the visual network (Fig. 3). IC 16 and IC 17 both belong to the primary visual cortex while IC 22 is belong to secondary visual cortex. We also found three other independent components, IC 10, IC 21 and IC 23 (correlation coefficients: 0.546, 0.361 and 0.348), were identified as the DMN (Fig. 3). Figure 3 also illustrates that there are some differences of functional connectivity in the visual network and the DMN between two groups.

Functional connectivity analysis

Two-sample t tests were performed to compare the independent components (subnetworks) of the visual network between two groups. We found that only the functional connectivity in occipital pole of IC 16 was significantly decreased ($p < 0.001$, cluster-wise FDR corrected) in POAG patients (Table 2 and Fig. 4), while no significant differences were found in IC 17 or IC 22 between two groups. When independent components of the default mode network between two groups were compared, no significant differences were found in any of three components in the default mode network, either.

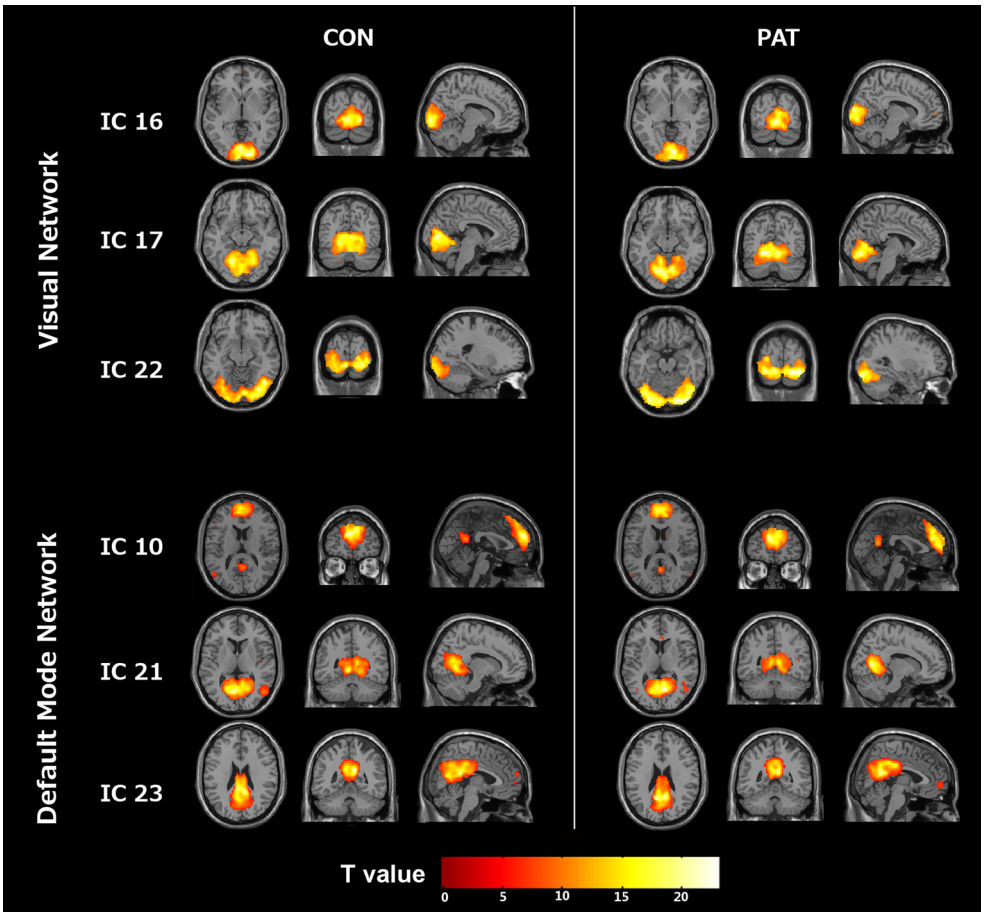

Fig. 3 Visual networks and default mode networks of normal controls and POAG patients (one-sample *t* test, $p < 0.05$, Bonferroni correction). CON: normal controls, PAT: POAG patients, IC x: independent component x obtained by Group ICA

Functional network connectivity analysis

We calculated the maximal lagged correlation coefficients between each two components in the visual network and the DMN. The coefficients between components of two groups are shown in Table 3. Normal controls show significantly positive correlation between each two subnetworks except for the coefficient of IC 22 – IC 23 (Column 3 in Table 3). All correlation coefficients between each two components are significantly positive in POAG patients (Column 4 in Table 3).

After performing the comparisons of coefficients between two groups, we found that i) two FNC coefficients within the visual network were significantly decreased (the coefficients of IC16 – IC17 and IC16 – IC22) in POAG patients (blue dashed line in Fig. 5); ii) the coefficients between each two components were not altered in the DMN; iii) there were three significantly altered correlations between two RSNs: the correlation coefficients of IC17 – IC23 and IC22 – IC23 were both increased (red solid line in Fig. 5) while the correlation coefficients of IC16 – IC21 was decreased in POAG patients (blue solid line in Fig. 5).

Correlation with clinical parameters

We correlated the functional connectivity of the occipital pole with clinical parameters in POAG patients and found that there was no significant correlation between the FC of

Table 2 Compared with normal controls, the functional connectivity of occipital pole in IC 16 of visual network significantly decreases in POAG patients ($p < 0.001$, cluster-wise FDR corrected)

Type	Anatomical location	Cluster size	MNI			T-value
			x (mm)	y (mm)	z (mm)	
CON > PAT	Occipital pole	68	12	-90	-9	4.45
			-3	-87	-12	3.60
			3	-93	-15	3.51

CON: normal controls, PAT: POAG patients

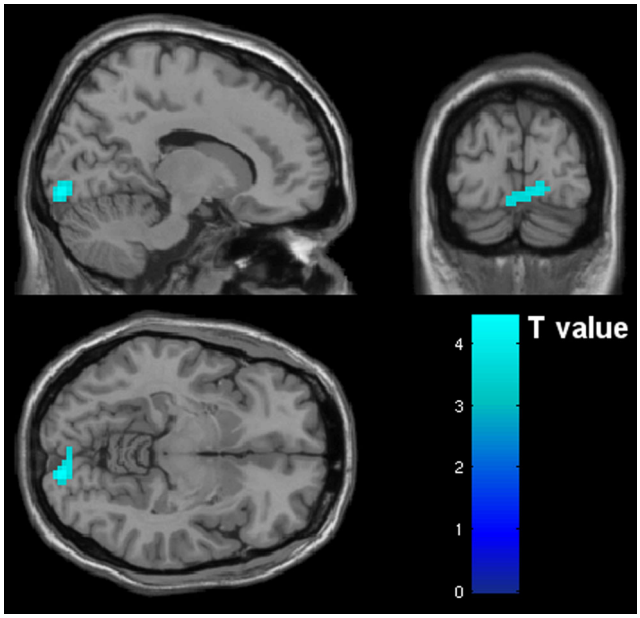

Fig. 4 Compared with normal controls, the functional connectivity of occipital pole in IC 16 of visual network significantly decreases in POAG patients ($p < 0.001$, cluster-wise FDR corrected)

occipital pole and any clinical parameter. The correlation coefficients between the abnormal FNC coefficients and the clinical parameters were calculated. Only the FNC coefficient between IC16 and IC21 was significantly positively correlated with the left visual field MD ($r = 0.707$, $p = 0.015$). The other abnormal FNC coefficients had no significant correlations with clinical parameters (details can be found in Table S2 in the supplementary).

Table 3 Comparison of FNC coefficients between normal controls and POAG patients

	IC - IC	CON	PAT	*p*-value	↑or↓
Visual - Visual	16–17	0.602*	0.390*	**0.017**	↓
	16–22	0.592*	0.381*	**0.007**	↓
	17–22	0.687*	0.560*	0.051	N.S.
DMN - DMN	10–21	0.414*	0.476*	0.372	N.S.
	10–23	0.483*	0.546*	0.280	N.S.
	21–23	0.466*	0.584*	0.070	N.S.
Visual - DMN	16–10	0.227*	0.228*	0.993	N.S.
	16–21	0.461*	0.275*	**0.011**	↓
	16–23	0.171*	0.238*	0.319	N.S.
	17–10	0.144*	0.148*	0.943	N.S.
	17–21	0.410*	0.295*	0.194	N.S.
	17–23	0.119*	0.272*	**0.019**	↑
	22–10	0.206*	0.312*	0.100	N.S.
	22–21	0.356*	0.313*	0.592	N.S.
	22–23	0.084	0.260*	**0.006**	↑

*represents significant correlation between components within each group ($p < 0.05$, FDR corrected). Bold numbers represent significant group differences of correlation between components ($p < 0.05$, uncorrected). IC - IC:the correlation between two components. CON: normal controls, PAT: POAG patients. Visual – Visual: correlation between two components within visual network. DMN – DMN: correlation between two components within DMN. Visual – DMN: correlation between the component in visual network and that in DMN. ↑: significantly increased correlation in POAG patients. ↓: significantly reduced correlation in POAG patients. N.S.: No significant alterations

Discussion

We investigated the alterations of FC and connections within and between the visual network and the DMN in POAG patients. Experimental results showed that in POAG patients (1) the FC in the occipital pole of the visual network were decreased while two of the three connections within the visual network were disrupted; (2) No disruptions were found in the FC in the DMN or the connections within DMN; (3) Two connections were increased and one connection was decreased between these two RSNs.

Frezztotti et al. applied the ICA method and found the altered FC in the occipital cortex of glaucoma patients (Frezzotti et al. 2014). Our study also found the FC in the occipital pole decreased in POAG patients, which is consistent with this study (Frezzotti et al. 2014). Occipital pole is located in Brodmann (BA) 17, the primary visual cortex, which receives the visual information from the lateral geniculate nucleus and sends the information to the secondary visual cortex. The decreased FC in the occipital pole of patients reflects the visual impairment in POAG patients. Furthermore, a seed-based FC analysis has also shown that the FC between BA17/18/19 and other regions was decreased in POAG patients (Dai et al. 2013), which also supports our result.

The human brain is organized according to two fundamental rules: the functional segregation and the functional integration (Zeki and Shipp 1988; Lee et al. 2003). The former means that different brain regions are responsible for different and relatively independent functions. The latter one means that different brain regions cooperate with each other to process information in perception and behavior. The connections between the subnetworks belonging to the same RSN reflect the functional segregation while the connections between subnetworks belonging to the different RSNs reflect the functional integration. We found that two of the three connections within the visual network were decreased in the POAG patients. These decreased connections correspond to the impairment of visual function of the visual network. This result may contribute to the smaller visual field MD in POAG patients. It is not surprising that the connections within the DMN are conserved in patients. The unchanged FC in the DMN was also reported in the Frezztotti's study of glaucoma (Frezzotti et al. 2014). In terms of the functional segregation, the DMN is usually thought to be related to attention and executive function (Fornito et al. 2012) as well as mind wandering (Baird

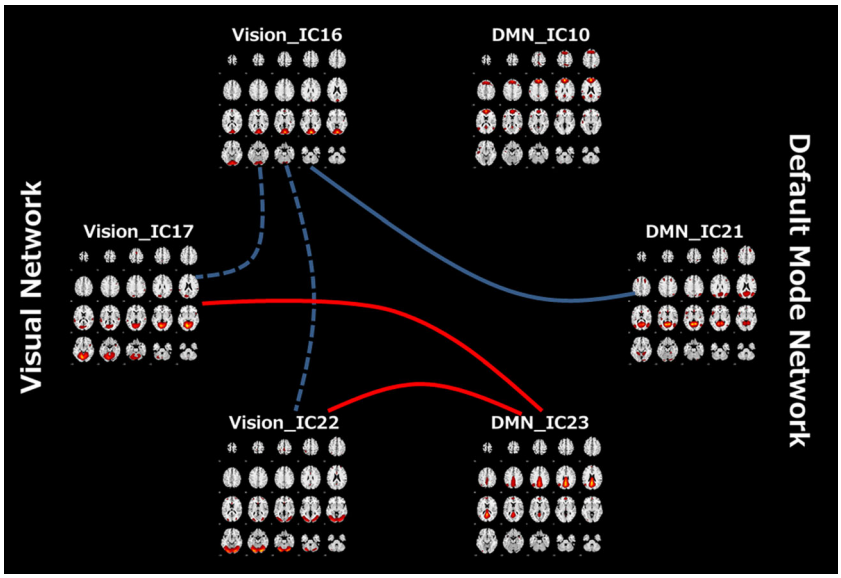

Fig. 5 Significant alterations of FNC coefficients between normal controls and POAG patients. Dashed lines represent significantly abnormal FNC within one subnetwork. Solid lines represent significantly abnormal FNC between two subnetworks. Red represents the significantly increased corresponding coefficient in POAG patients. Blue represents the significantly decreased corresponding coefficient in POAG patients

et al. 2012). The DMN has little correlation with visual function, and the visual impairment in glaucoma has limited influence on the connections within the DMN.

The connections between the visual network and the DMN reflect the functional integration of these two RSNs. Among the connections between the subnetworks belonging to different RSNs, we found two increased connections (IC17 – IC23 and IC22 – IC23) and one decreased connection (IC16 – IC21) in POAG patients. Some people may argue that this reorganization may be related to more general functions, such as eye movement control and attention, rather than vision-related diseases. This claim is untenable because we did not observe any FC changes within the DMN. On the contrary, the FC changes between the visual network and DMN are observed. Therefore, it is logical to infer that only the vision-related diseases are related to this reorganization. More importantly, special attention should be paid to the deceased IC16 – IC 21 connection due to its significant correlation with the visual field MD in the patient group. This finding suggests that this connection can reflect glaucoma severity.

In terms of the correlations between the changed FNC and clinical parameters, we would like to emphasize the following points. Firstly, correction is usually not adopted when making correlations between brain change and clinical parameters. Secondly, many previous studies (T. Li et al. 2015; Dai et al. 2013; Lin et al. 2012; Wang et al. 2014) have applied rsfMRI to investigating the visual functions, which suggest that rsfMRI is effective and useful to unravel some pathological mechanisms of vision-related diseases. In terms of MRI connections at rest, they are also widely adopted in investigating various vision-related diseases (Ding et al. 2013; Dai et al. 2013). Therefore, we applied rsfMRI to investigating the reorganization of visual functions in our method. Thirdly, we admit that only one correlation is found in our research. However, this single correlation can shed light on the importance of the reorganization of resting state networks in glaucoma mechanism. Finally, we would like to emphasize that the goal of using rest-state fMRI in our research is not to compare the changes on the visual functions; instead, our goal is to investigate the reorganization in the brain. Resting-state fMRI is the basic state of brain functions, which, therefore, is suitable to be applied to our research. Some previous studies (Bola et al. 2014; Bola et al. 2015) showed that EEG-recorded functional connectivity changed after optic nerve damage at rest, and the altered functional connectivity had a significant correlation with visual parameters. Therefore, we will combine the analysis on both fMRI and EEG at rest in our future research. Besides, considering that MRI represents BOLD activation whereas EEG represents electrophysiological activation/connectivity, the studies at rest are also needed to be combined with a visually evoked response analysis as done in normal subjects (W. Chen et al. 1998; Schwartz et al. 2005; Bressler et al. 2013) or with brain evoked network activation (Bola and Sabel 2015).

We also noticed that the decreased connection between the DMN and the visual network is only significantly correlated with the left visual field MD, but not with the right one. We conjecture that this is probably due to the lateralization property of the brain. Actually, our previous study (Wang et al. 2016a, b) has also found similar phenomena in LGN. Here, the volume of the left LGN is significantly larger than that of the right LGN both in healthy subjects and glaucoma patients. We will further investigate the underlying reasons in future studies.

The result that two connections within the visual network are decreased in POAG patients is different from Dai's study (Dai et al. 2013). Specifically, Dai et al. applied the seed-based

analysis in the study and chose representative seeds (circular regions) from BA17, BA18, and BA19, respectively. They reported that no alterations were found in the connections between each two regions. But we think the main reason is that the seed-based analysis only chooses the representative ROIs and thereby ignores other regions in the RSN. Furthermore, the seed-based approach cannot eliminate the noise effect even though noise correction is performed (Murphy et al. 2009). In contrast, ICA is totally a data-driven approach and does not need prior information. The fMRI signal is regarded as a mixing of signals of different ICs (McKeown et al. 1998). ICA divides the fMRI signal into several ICs and the corresponding time courses, overcoming the limitations of the seed-based approach. Therefore, the ICA method is superior to the seed-based method.

This study had several limitations. Firstly, the results were based on a relatively small sample size, which may limit the power of statistical comparisons. Secondly, the components extracted by ICA method did not exactly correspond to the anatomical structures. One anatomical structure may be divided into several components. Similarly, one component may include several anatomical structures. It is not easy to exactly explain the abnormal connections derived from which anatomical structures. Thirdly, this study mainly focused on the visual network and the DMN, the potential alterations exist in other RSNs. Fourthly, correlation analysis does not allow to differentiate cause and effect of behavioral and physiological measures, i.e. the connectivity change and vision loss. The causal relationship between the changes and the vision loss should be investigated in the future.

In conclusion, the functional connectivity in the occipital pole was found to be reduced in the patient group. We also found that two connections within the visual network were significantly reduced while three connections between the visual network and the DMN were significantly altered in patients. The decreased connection between the subnetworks belonging to these two RSNs was positively correlated with the visual field MD. These findings may promote the understanding of glaucoma via clarifying the importance of the reorganization of RSNs in glaucoma mechanism.

Acknowledgments This work was supported by National Natural Science Foundation of China (61271151, 91520202, and 81571649) and Youth Innovation Promotion Association CAS.

Compliance with ethical standards

Disclosures Author Jieqiong Wang, Author Ting Li, Author Peng Zhou, Author Ningli Wang, Author Junfang Xian, Author Huiguang He declare that they have no conflict of interest.

All procedures followed were in accordance with the ethical standards of the responsible committee on human experimentation (institutional and national) and with the Helsinki Declaration of 1975, and the applicable revisions at the time of the investigation. Informed consent was obtained from all patients for being included in the study.

References

Alba, C., Vidal, L., Diaz, F., Villena, A., & de Vargas, I. P. (2004). Ultrastructural and quantitative age-related changes in capillaries of the dorsal lateral geniculate nucleus. *Brain Research Bulletin, 64*(2), 145–153. doi:10.1016/j.brainresbull.2004.06.006.

Baird, B., Smallwood, J., Mrazek, M. D., Kam, J. W., Franklin, M. S., & Schooler, J. W. (2012). Inspired by distraction: mind wandering facilitates creative incubation. *Psychological Science, 23*(10), 1117–1122. doi:10.1177/0956797612446024.

Bell, A. J., & Sejnowski, T. J. (1995). An information maximization approach to blind separation and blind deconvolution. *Neural Computation, 7*(6), 1129–1159. doi:10.1162/Neco.1995.7.6.1129.

Bola, M., & Sabel, B. A. (2015). Dynamic reorganization of brain functional networks during cognition. *NeuroImage, 114*, 398–413. doi:10.1016/j.neuroimage.2015.03.057.

Bola, M., Gall, C., Moewes, C., Fedorov, A., Hinrichs, H., & Sabel, B. A. (2014). Brain functional connectivity network breakdown and restoration in blindness. [randomized controlled trial research support, non-U.S. Gov't]. *Neurology, 83*(6), 542–551. doi:10.1212/WNL.0000000000000672.

Bola, M., Gall, C., & Sabel, B. A. (2015). Disturbed temporal dynamics of brain synchronization in vision loss. *Cortex, 67*, 134–146. doi:10.1016/j.cortex.2015.03.020.

Bressler, D. W., Fortenbaugh, F. C., Robertson, L. C., & Silver, M. A. (2013). Visual spatial attention enhances the amplitude of positive and negative fMRI responses to visual stimulation in an eccentricity-dependent manner. *Vision Research, 85*, 104–112. doi:10.1016/j.visres.2013.03.009.

Calhoun, V. D., Adali, T., Pearlson, G. D., & Pekar, J. J. (2001). A method for making group inferences from functional MRI data using independent component analysis. *Human Brain Mapping, 14*(3), 140–151.

Chen, W., Kato, T., Zhu, X. H., Strupp, J., Ogawa, S., & Ugurbil, K. (1998). Mapping of lateral geniculate nucleus activation during visual stimulation in human brain using fMRI. [Clinical Trial Research Support, U.S. Gov't, P.H.S.]. *Magn Reson Med., 39*(1), 89–96.

Chen, W. W., Wang, N., Cai, S., Fang, Z., Yu, M., Wu, Q., et al. (2013). Structural brain abnormalities in patients with primary open-angle glaucoma: a study with 3 T MR imaging. [comparative study research support, non-U.S. Gov't]. *Investigative Ophthalmology & Visual Science, 54*(1), 545–554. doi:10.1167/iovs.12-9893.

Dai, H., Mu, K. T., Qi, J. P., Wang, C. Y., Zhu, W. Z., Xia, L. M., et al. (2011). Assessment of lateral geniculate nucleus atrophy with 3 T MR imaging and correlation with clinical stage of glaucoma. [controlled clinical trial]. AJNR. *American Journal of Neuroradiology, 32*(7), 1347–1353. doi:10.3174/ajnr.A2486.

Dai, H., Morelli, J. N., Ai, F., Yin, D., Hu, C., Xu, D., et al. (2013). Resting-state functional MRI: functional connectivity analysis of the visual cortex in primary open-angle glaucoma patients. [research support, non-U.S. Gov't]. *Human Brain Mapping, 34*(10), 2455–2463. doi:10.1002/hbm.22079.

Damoiseaux, J. S., Rombouts, S. A., Barkhof, F., Scheltens, P., Stam, C. J., Smith, S. M., et al. (2006). Consistent resting-state networks across healthy subjects. *Proceedings of the National Academy of Sciences of the United States of America, 103*(37), 13848–13853. doi:10.1073/pnas.0601417103.

Ding, K., Liu, Y., Yan, X., Lin, X., & Jiang, T. (2013). Altered functional connectivity of the primary visual cortex in subjects with amblyopia. *Neural Plasticity, 2013*, 8. doi:10.1155/2013/612086.

Erhardt, E. B., Rachakonda, S., Bedrick, E. J., Allen, E. A., Adali, T., & Calhoun, V. D. (2011). Comparison of multi-subject ICA methods for analysis of fMRI data. *Human Brain Mapping, 32*(12), 2075–2095. doi:10.1002/hbm.21170.

Fornito, A., Harrison, B. J., Zalesky, A., & Simons, J. S. (2012). Competitive and cooperative dynamics of large-scale brain functional networks supporting recollection. *Proceedings of the National Academy of Sciences of the United States of America, 109*(31), 12788–12793. doi:10.1073/pnas.1204185109.

Frezzotti, P., Giorgio, A., Motolese, I., De Leucio, A., Iester, M., Motolese, E., et al. (2014). Structural and functional brain changes beyond visual system in patients with advanced glaucoma. *PloS One, 9*(8), e105931. doi:10.1371/journal.pone.0105931.

Garaci, F. G., Bolacchi, F., Cerulli, A., Melis, M., Spano, A., Cedrone, C., et al. (2009). Optic nerve and optic radiation neurodegeneration in patients with glaucoma: in vivo analysis with 3-T diffusion-tensor MR imaging. *Radiology, 252*(2), 496–501. doi:10.1148/radiol.2522081240.

Gentili, C., Ricciardi, E., Gobbini, M. I., Santarelli, M. F., Haxby, J. V., Pietrini, P., et al. (2009). Beyond amygdala: default mode network activity differs between patients with social phobia and healthy controls. *Brain Research Bulletin, 79*(6), 409–413. doi:10.1016/j.brainresbull.2009.02.002.

Greicius, M. D., Krasnow, B., Reiss, A. L., & Menon, V. (2003). Functional connectivity in the resting brain: a network analysis of the default mode hypothesis. *Proceedings of the National Academy of Sciences of the United States of America, 100*(1), 253–258. doi:10.1073/pnas.0135058100.

Gupta, N., & Yucel, Y. H. (2007). Glaucoma as a neurodegenerative disease. *Current Opinion in Ophthalmology, 18*(2), 110–114. doi:10.1097/Icu.0b013e3280895aea.

Gupta, N., Ang, L. C., de Tilly, L. N., Bidaisee, L., & Yucel, Y. H. (2006a). Human glaucoma and neural degeneration in intracranial optic nerve, lateral geniculate nucleus, and visual cortex. *British Journal of Ophthalmology, 90*(6), 674–678. doi:10.1136/bjo.2005.086769.

Jafri, M. J., Pearlson, G. D., Stevens, M., & Calhoun, V. D. (2008). A method for functional network connectivity among spatially independent resting-state components in schizophrenia. *NeuroImage, 39*(4), 1666–1681. doi:10.1016/j.neuroimage.2007.11.001.

Joel, S. E., Caffo, B. S., Zijl, P. C. M., & Pekar, J. J. (2011). On the relationship between seed-based and ICA-based measures of functional connectivity. *Magnetic Resonance in Medicine, 66*(3), 644–657. doi:10.1002/mrm.22818.

Lee, L., Harrison, L. M., & Mechelli, A. (2003). A report of the functional connectivity workshop, Dusseldorf 2002. *NeuroImage, 19*(2 Pt 1), 457–465.

Li, Y. O., Adali, T., & Calhoun, V. D. (2007). Estimating the number of independent components for functional magnetic resonance imaging data. *Human Brain Mapping, 28*(11), 1251–1266. doi:10.1002/hbm.20359.

Li, T., Liu, Z., Li, J., Liu, Z., Tang, Z., Xie, X., et al. (2015). Altered amplitude of low-frequency fluctuation in primary open-angle glaucoma: a resting-state FMRI study. *Investigative Ophthalmology & Visual Science, 56*(1), 322–329. doi:10.1167/iovs.14-14974.

Lin, X. M., Ding, K., Liu, Y., Yan, X. H., Song, S. J., & Jiang, T. Z. (2012). Altered spontaneous activity in anisometropic amblyopia subjects: revealed by resting-state fMRI. *PloS One, 7*(8). doi:10.1371/journal.pone.0043373.

McKeown, M. J., Makeig, S., Brown, G. G., Jung, T. P., Kindermann, S. S., Bell, A. J., et al. (1998). Analysis of fMRI data by blind separation into independent spatial components. *Human Brain Mapping, 6*(3), 160–188.

Murphy, K., Birn, R. M., Handwerker, D. A., Jones, T. B., & Bandettini, P. A. (2009). The impact of global signal regression on resting state correlations: are anti-correlated networks introduced? *NeuroImage, 44*(3), 893–905. doi:10.1016/j.neuroimage.2008.09.036.

Ongur, D., Lundy, M., Greenhouse, I., Shinn, A. K., Menon, V., Cohen, B. M., et al. (2010). Default mode network abnormalities in bipolar disorder and schizophrenia. *Psychiatry Research, 183*(1), 59–68. doi:10.1016/j.pscychresns.2010.04.008.

Raichle, M. E., MacLeod, A. M., Snyder, A. Z., Powers, W. J., Gusnard, D. A., & Shulman, G. L. (2001). A default mode of brain function. *Proceedings of the National Academy of Sciences of the United States of America, 98*(2), 676–682. doi:10.1073/pnas.98.2.676.

Schwartz, S., Vuilleumier, P., Hutton, C., Maravita, A., Dolan, R. J., & Driver, J. (2005). Attentional load and sensory competition in human vision: modulation of fMRI responses by load at fixation during task-irrelevant stimulation in the peripheral visual field. *Cerebral Cortex, 15*(6), 770–786. doi:10.1093/cercor/bhh178.

Shirer, W. R., Ryali, S., Rykhlevskaia, E., Menon, V., & Greicius, M. D. (2012). Decoding subject-driven cognitive states with whole-brain connectivity patterns. *Cerebral Cortex, 22*(1), 158–165. doi:10.1093/Cercor/Bhr099.

Song, Y., Mu, K., Wang, J., Lin, F., Chen, Z., Yan, X., et al. (2014). Altered spontaneous brain activity in primary open angle glaucoma: a resting-state functional magnetic resonance imaging study. [Comparative Study Research Support, Non-U.S. Gov't]. *PLoS One, 9*(2), e89493, doi:10.1371/journal.pone.0089493.

Tian, L., Ren, J., & Zang, Y. (2012). Regional homogeneity of resting state fMRI signals predicts stop signal task performance. *NeuroImage, 60*(1), 539–544. doi:10.1016/j.neuroimage.2011.11.098.

van de Ven, V. G., Formisano, E., Prvulovic, D., Roeder, C. H., & Linden, D. E. J. (2004). Functional connectivity as revealed by spatial independent component analysis of fMRI measurements during rest. *Human Brain Mapping, 22*(3), 165–178. doi:10.1002/hbm.20022.

van den Heuvel, M. P., & Hulshoff Pol, H. E. (2010). Exploring the brain network: a review on resting-state fMRI functional connectivity. [review]. *European Neuropsychopharmacology, 20*(8), 519–534. doi:10.1016/j.euroneuro.2010.03.008.

Vidal, L., Ruiz, C., Villena, A., Diaz, F., & Perez de Vargas, I. (2004). Quantitative age-related changes in dorsal lateral geniculate nucleus relay neurons of the rat. *Neuroscience Research, 48*(4), 387–396. doi:10.1016/j.neures.2003.12.004.

von dem Hagen, E. A. H., Stoyanova, R. S., Baron-Cohen, S., & Calder, A. J. (2012). Reduced functional connectivity within and between 'social'resting state networks in autism spectrum conditions. *Social Cognitive and Affective Neuroscience, 8*(6), 694–701. doi:10.1093/scan/nss053.

Wang, T. Y., Li, Q., Guo, M. X., Peng, Y. M., Li, Q. J., Qin, W., et al. (2014). Abnormal functional connectivity density in children with anisometropic amblyopia at resting-state. *Brain Research, 1563*, 41–51. doi:10.1016/J.Brainres.2014.03.015.

Wang, J. Q., Li, T., Sabel, B. A., Chen, Z. Q., Wen, H. W., Li, J. H., et al. (2016a). Structural brain alterations in primary open angle glaucoma: a 3 T MRI study. *Scientific Reports, 6*. doi:10.1038/Srep18969.

Wang, J., Li, T., Wang, N., Xian, J., & He, H. (2016b). Graph theoretical analysis reveals the reorganization of the brain network pattern in primary open angle glaucoma patients. *European Radiology*. doi:10.1007/s00330-016-4221-x.

Williams, A. L., Lackey, J., Wizov, S. S., Chia, T. M., Gatla, S., Moster, M. L., et al. (2013). Evidence for widespread structural brain changes in glaucoma: a preliminary voxel-based MRI study. [research support, non-U.S. Gov't]. *Investigative Ophthalmology & Visual Science, 54*(8), 5880–5887. doi:10.1167/iovs.13-11776.

Yan, C. G., & Zang, Y. F. (2010). DPARSF: a MATLAB toolbox for "pipeline" data analysis of resting-state fMRI. *Frontiers in Systems Neuroscience, 4*. doi:10.3389/fnsys.2010.00013.

Yu, L., Xie, B., Yin, X., Liang, M., Evans, A. C., Wang, J., et al. (2013). Reduced cortical thickness in primary open-angle glaucoma and its relationship to the retinal nerve fiber layer thickness. [Research Support, Non-U.S. Gov't]. *PLoS One, 8*(9), e73208, doi:10.1371/journal.pone.0073208.

Zeki, S., & Shipp, S. (1988). The functional logic of cortical connections. *Nature, 335*(6188), 311–317. doi:10.1038/335311a0.